IEICE TRANSACTIONS

on Communications

VOL. E99-B NO. 11
NOVEMBER 2016

A PUBLICATION OF THE COMMUNICATIONS SOCIETY

The Institute of Electronics, Information and Communication Engineers
Kikai-Shinko-Kaikan Bldg., 5-8, Shibakoen 3chome, Minato-ku, TOKYO, 105-0011 JAPAN

IEICE TRANS. COMMUN., VOL.E99–B, NO.11 NOVEMBER 2016

PAPER

Relating Crosstalk to Plane-Wave Field-to-Wire Coupling

Flavia GRASSI[†a)], **Giordano SPADACINI**[†b)], **Keliang YUAN**[†], *Nonmembers*, *and* **Sergio A. PIGNARI**[†c)], *Member*

SUMMARY In this work, a novel formulation of crosstalk (XT) is developed, in which the perturbation/loading effect that the generator circuit exerts on the passive part of the receptor circuit is elucidated. Practical conditions (i.e., weak coupling and matching/mismatching of the generator circuit) under which this effect can be neglected are then discussed and exploited to develop an alternative radiated susceptibility (RS) test procedure, which resorts to crosstalk to induce at the terminations of a cable harness the same disturbance that would be induced by an external uniform plane-wave field. The proposed procedure, here developed with reference to typical RS setups foreseen by Standards of the aerospace sector, assures equivalence with field coupling without *a priori* knowledge and/or specific assumptions on the units connected to the terminations of the cable harness. Accuracy of the proposed scheme of equivalence is assessed by virtual experiments carried out in a full-wave simulation environment.

key words: *aerospace standards, crosstalk, field-to-wire coupling, radiated susceptibility, weak coupling assumption*

1. Introduction

Crosstalk (XT) is a distributed coupling phenomenon between two adjacent wiring structures, through which a generator circuit induces undesired voltages and currents at the terminations of a receptor circuit by means of inductive and capacitive mutual coupling. Modeling strategies and best-practice for XT reduction are very similar to those adopted for field-to-wire coupling (FC), which is also a distributed coupling phenomenon due to an external electromagnetic (EM) field impinging on a victim wiring structure. The close analogy, [1], between these two coupling phenomena suggests the possibility of resorting to crosstalk to develop alternative procedures for radiated susceptibility (RS) testing of systems involving interconnecting wiring harness. This could be particularly appealing for pre-compliance verification of units and sub-units to be assembled in complex systems (such as in cars, aircrafts, etc.). Indeed, since XT is a near-field phenomenon of coupling, XT-based procedures could avoid the use of large and expensive test facilities, as traditionally required for RS testing. On the other hand, several examples of alternative RS test procedures targeted to this goal can be found in the literature. They are mainly based on the use of injection devices, such as bulk current injection probes [2], [3]. However, in those procedures, the not-negligible effect of loading exerted by the injection device on the harness under test may limit test practicality, since the proposed schemes of equivalence inherently require accurate knowledge of the networks connected to the terminations of the victim circuit. In this respect, one of the noteworthy advantages of resorting to XT stems from the theoretical possibility of enforcing equivalence with FC without any need for *a priori* knowledge of the receptor loads. However, this result can be achieved as long as the perturbation effect that the generator circuit plays on the passive part of the receptor (i.e., its loading effect) is negligible.

This work investigates this specific aspect by developing a novel frequency-domain formulation of XT, in which the effect of loading/perturbation exerted by the generator circuit on the harness under test (victim circuit) is rigorously pointed out by a suitable augmented circuit representation of the victim circuit. It is shown that if the two circuits are weakly coupled, the condition of matching at the terminations of the generator circuit, exploited in [4], can be relaxed, and negligibility of the loading effect onto the victim circuit can be achieved also for practical impedance values at the terminations of the generator circuit (e.g., 50 Ω impedances). Based on this finding, a more general and feasible scheme of equivalence is proposed and validated by full-wave numerical simulation. The proposed results overcome previous attempts available in the literature, whose applicability was limited to specific incidence conditions of the EM field [5], [6], or by stringent requirements (i.e., conditions of matching) on the terminations of the circuit to be used in order to induce XT in the victim circuit, [4]. Also, it is shown that this new equivalence scheme offers advantages in terms of the forward power required to carry out the test. Despite the results derived in this paper refer to incidence conditions foreseen by aerospace Standards [7], [8], the theory here developed assures equivalence between XT and FC for any condition of incidence of the impinging EM field. Additionally, although validated for resistive loads only, it holds for whatever loads, even non-linear, connected to the terminations of the receptor circuit.

The paper is organized as follows. In Sect. 2, a novel XT formulation is introduced and used to discuss negligibility of the loading effect. In Sect. 3, conditions of equivalence with FC are derived for the specific test cases foreseen by aerospace Standards. In Sect. 4, the proposed scheme of equivalence is validated by transmission line (TL)-based prediction models and by full-wave simulations carried out

Manuscript received January 18, 2016.
Manuscript revised April 18, 2016.
Manuscript publicized May 25, 2016.

[†]The authors are with Department of Electronics, Information and Bioengineering, Politecnico di Milano, Milan, Italy.
a) E-mail: flavia.grassi@polimi.it
b) E-mail: giordano.spadacini@polimi.it
c) E-mail: sergio.pignari@polimi.it

DOI: 10.1587/transcom.2016EBP3027

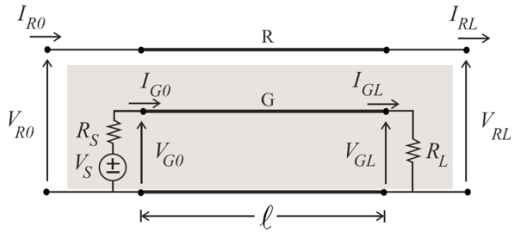

Fig. 1 Canonical three-wire TL structure used for XT modeling.

by the Method of Moments (MoM), [9]. Conclusions are eventually drawn in Sect. 5.

2. Crosstalk Model

In order to develop a scheme of equivalence holding for whatever loads (linear or non-linear) connected to the terminations of the receptor circuit, equivalence between FC and XT will be here enforced in terms of open-ended equivalent circuits at the output ports of the receptor. To this end, the canonical three-wire TL structure in Fig. 1 is considered [10], [11], where G denotes the generator circuit and R the receptor. In this structure, the two circuits run parallel above a metallic ground plane and are kept at a constant distance d. The generator is driven from the left termination by a non-ideal voltage source with parameters V_S and R_S, the right termination being loaded by a resistor R_L. With reference to the open-ended equivalent representation of the circuit victim of radiated interference in Appendix A, the objective here is to include the effects due to the generator circuit into the equations relating voltages (V_{R0}, V_{RL}) and currents (I_{R0}, I_{RL}) at the terminations of the receptor, so to discuss the conditions under which the two representations can be made equivalent at the output ports.

2.1 Receptor Equivalent Circuit

By virtue of TL theory, the relationships between the voltage ($\boldsymbol{V}_0, \boldsymbol{V}_L$) and ($\boldsymbol{I}_0, \boldsymbol{I}_L$) current vectors at the output and input ports of the three-wire TL in Fig. 1 can be written in matrix notation as

$$\begin{pmatrix} \boldsymbol{V}_L \\ \boldsymbol{I}_L \end{pmatrix} = \begin{bmatrix} \cosh(\gamma_0 L)\boldsymbol{I} & -\sinh(\gamma_0 L)\boldsymbol{Z}_C \\ -\sinh(\gamma_0 L)\boldsymbol{Z}_C^{-1} & \cosh(\gamma_0 L)\boldsymbol{I} \end{bmatrix} \cdot \begin{pmatrix} \boldsymbol{V}_0 \\ \boldsymbol{I}_0 \end{pmatrix}, \tag{1}$$

where $\boldsymbol{I}$ denotes the 2×2 identity matrix, $\gamma_0 = j\omega/c_0$ denotes the propagation constant (c_0 being the speed of light in free space), $\boldsymbol{V}_0 = [V_{G0}, V_{R0}]^T$, $\boldsymbol{V}_L = [V_{GL}, V_{RL}]^T$, $\boldsymbol{I}_0 = [I_{G0}, I_{R0}]^T$, $\boldsymbol{I}_L = [I_{GL}, I_{RL}]^T$ are 2×1 vectors of voltages and currents at the input and output ports, respectively, and

$$\boldsymbol{Z}_C = \begin{bmatrix} Z_G & Z_m \\ Z_m & Z_R \end{bmatrix} \tag{2}$$

is the characteristic impedance matrix. In the absence of losses and dielectric material, $\boldsymbol{Z}_C$ takes the expression: $\boldsymbol{Z}_C = c_0 \boldsymbol{L}$, where $\boldsymbol{L}$ is the per-unit-length (p.u.l.) inductance matrix associated with the cross-section of the TL in Fig. 1. Hence, the inverse of this matrix can be written as:

$$\boldsymbol{Z}_C^{-1} = c_0^{-1}\boldsymbol{L}^{-1} = \frac{1}{1-k^2}\begin{bmatrix} 1/Z_G & -k^2/Z_m \\ -k^2/Z_m & 1/Z_R \end{bmatrix}, \tag{3}$$

where Z_G, Z_R represent the characteristic impedances of the generator and receptor circuits, respectively, whereas the mutual impedance Z_m is related to the coupling coefficient k in (3) as: $k = Z_m/\sqrt{Z_G Z_R}$, [10], [11]. In order to obtain an equivalent representation at the output ports of the receptor, equations in (1) are made explicit as

$$\begin{pmatrix} V_{GL} \\ V_{RL} \\ I_{GL} \\ I_{RL} \end{pmatrix} = \begin{bmatrix} \phi_1 & 0 & \phi_2 & \phi_3 \\ 0 & \phi_1 & \phi_3 & \phi_4 \\ \phi_5 & \phi_6 & \phi_1 & 0 \\ \phi_6 & \phi_7 & 0 & \phi_1 \end{bmatrix} \cdot \begin{pmatrix} V_{G0} \\ V_{R0} \\ I_{G0} \\ I_{R0} \end{pmatrix}, \tag{4}$$

where: $\phi_1 = \cosh(\gamma_0\ell)$, $\phi_{2,3,4} = -\sinh(\gamma_0\ell)Z_{G,m,R}$, $\phi_{5,6,7} = -\sinh(\gamma_0\ell)/Z_{G,m,R}/(1-k^2)$, and subsequently combined with the port-constraints at the terminations of the generator circuit, i.e.,

$$V_{G0} = V_S - \alpha Z_G I_{G0}, \text{ with } \alpha = R_S/Z_G, \tag{5}$$

$$V_{GL} = \beta Z_G I_{GL}, \text{ with } \beta = R_L/Z_G. \tag{6}$$

This allows including effects due to the generator into the equivalent circuit of the receptor, whose output voltages and currents can be now cast as:

$$\begin{pmatrix} V_{RL} \\ I_{RL} \end{pmatrix} = \underbrace{\begin{bmatrix} \Phi_{11} & \Phi_{12} \\ \Phi_{21} & \Phi_{22} \end{bmatrix}}_{\boldsymbol{\Phi}} \cdot \begin{pmatrix} V_{R0} \\ I_{R0} \end{pmatrix} + \begin{pmatrix} V_{XT} \\ I_{XT} \end{pmatrix}, \tag{7}$$

$$\Phi_{11} = \phi_1 + \frac{\beta Z_G \phi_3 \phi_6}{D_1}, \quad \Phi_{22} = \phi_1 + \frac{\alpha Z_G \phi_3 \phi_6}{D_1}, \tag{8}$$

$$\Phi_{12} = \phi_4 - \frac{\phi_3^2}{D_1}, \quad \Phi_{21} = \phi_7 - \frac{\alpha\beta Z_G^2 \phi_6^2}{D_1}, \tag{9}$$

$$\frac{V_{XT}}{V_S} = \phi_3 \frac{\beta Z_G \phi_5 - \phi_1}{D_1}, \quad \frac{I_{XT}}{V_S} = \phi_6 \left(1 - \alpha Z_G \frac{\beta Z_G \phi_5 - \phi_1}{D_1}\right), \tag{10}$$

and $D_1 = -\phi_1(\alpha+\beta)Z_G + \phi_2 + \alpha\beta Z_G^2 \phi_5$.

Through some cumbersome algebra, here omitted for the sake of brevity, the port-constraints in (7)–(10) can be re-written as

$$\begin{pmatrix} I_{R0} \\ -I_{RL} \end{pmatrix} = \underbrace{\begin{bmatrix} y_{11} & y_{12} \\ y_{12} & y_{22} \end{bmatrix}}_{\boldsymbol{Y}} \cdot \begin{pmatrix} V_{R0} - V_{XT0} \\ V_{RL} - V_{XTL} \end{pmatrix}, \tag{11}$$

which allow the circuit representation of the receptor circuit shown in Fig. 2. This model clearly puts in evidence the twofold nature of crosstalk coupling. As a matter of fact, since crosstalk is inherently a near-field phenomenon, both the active and passive parts of the receptor circuit are affected. Concerning the active part, effects due to crosstalk can be modeled by two voltage sources connected to the terminations of the receptor circuit and taking the analytical

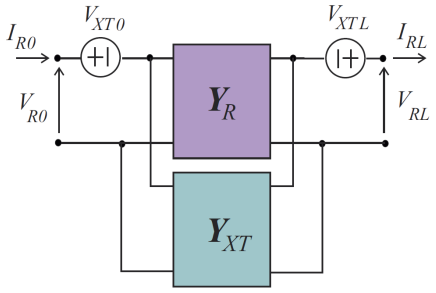

Fig. 2 Equivalent representation of the receptor circuit where effects due to the generator circuit are included by means of (a) two voltage sources V_{XT0}, V_{XTL} (active part) and (b) matrix $\boldsymbol{Y}_{XT}$ (passive part).

expressions:

$$V_{XT0} = \frac{Z_m}{Z_G} \frac{\beta \cosh(\gamma_0 \ell) + \sinh(\gamma_0 \ell)}{(\alpha + \beta)\cosh(\gamma_0 \ell) + (1 + \alpha\beta)\sinh(\gamma_0 \ell)} V_s, \tag{12}$$

$$V_{XTL} = \frac{Z_m}{Z_G} \frac{\beta}{(\alpha + \beta)\cosh(\gamma_0 \ell) + (1 + \alpha\beta)\sinh(\gamma_0 \ell)} V_s. \tag{13}$$

Conversely, the passive part of the model can be conveniently interpreted as the parallel connection of two admittance matrices as:

$$\boldsymbol{Y} = \boldsymbol{Y}_R + \boldsymbol{Y}_{XT}. \tag{14}$$

In (14), matrix $\boldsymbol{Y}_R$ represents the admittance matrix of the receptor circuit in the absence of the generator, that is

$$\boldsymbol{Y}_R = \begin{bmatrix} y_{11}^R & y_{12}^R \\ y_{12}^R & y_{11}^R \end{bmatrix} = \frac{1}{Z_R \sinh(\gamma_o \ell)} \begin{bmatrix} \cosh(\gamma_0 \ell) & -1 \\ -1 & \cosh(\gamma_0 \ell) \end{bmatrix}, \tag{15}$$

whereas matrix

$$\boldsymbol{Y}_{XT} = \begin{bmatrix} y_{11}^{XT} & y_{12}^{XT} \\ y_{12}^{XT} & y_{22}^{XT} \end{bmatrix}, \tag{16}$$

accounts for the effect of "loading", i.e., of perturbation, that the presence of the generator circuit exerts on the p.u.l. parameters of the receptor circuit by virtue of the close proximity between the two circuits. Analytical expressions for the entries in (16) are given by:

$$y_{11}^{XT} = k^2[\beta \sinh(\gamma_0 \ell) + (1 - k^2)\cosh(\gamma_0 \ell)]/D_2, \tag{17}$$

$$y_{22}^{XT} = k^2[\alpha \sinh(\gamma_0 \ell) + (1 - k^2)\cosh(\gamma_0 \ell)]/D_2, \tag{18}$$

$$y_{12}^{XT} = -k^2(1 - k^2)/D_2, \tag{19}$$

$$D_2 = [(1 - k^2)[(\alpha + \beta)\cosh(\gamma_0 \ell) + \sinh(\gamma_0 \ell)(1 - k^2)] + \alpha\beta \sinh(\gamma_0 \ell)]Z_R, \tag{20}$$

and show that the receptor behaves as a non-symmetrical two-port network as long as $\alpha \neq \beta$.

2.2 Perturbation of the Passive Part

The circuit interpretation in Fig. 2 allows a deep insight into the effect of perturbation exerted by the generator onto the passive part of the receptor, as a fundamental step towards enforcing equivalence with FC. To this end, we will hereinafter assume equal loads connected to the terminations of the generator, i.e., $\beta = \alpha$. Indeed, besides being easy to realize, this condition allows the passive part of the receptor circuit in Fig. 2 going back to being symmetric, that is $\tilde{y}_{11}^{XT} = \tilde{y}_{22}^{XT}$. Under this simplifying assumption, the entries of matrix $\boldsymbol{Y}_{XT}$ simplify to

$$\tilde{y}_{11}^{XT} = \tilde{y}_{22}^{XT} = \frac{k^2}{Z_R} \frac{\alpha \sinh(\gamma_0 \ell) + \cosh(\gamma_0 \ell)}{2\alpha \cosh(\gamma_0 \ell) + (1 + \alpha^2)\sinh(\gamma_0 \ell)}, \tag{21}$$

$$\tilde{y}_{12}^{XT} = -\frac{k^2/Z_R}{2\alpha \cosh(\gamma_0 \ell) + (1 + \alpha^2)\sinh(\gamma_0 \ell)}, \tag{22}$$

and can be directly compared versus those of $\boldsymbol{Y}_R$ and $\boldsymbol{Y}$ in (14) for different values of α and k. To this end, an exemplifying wiring structure composed of two bare wires with radius $r_w = 0.5$ mm, length $\ell = 1$ m, and height above ground $h = 50$ mm is considered. Two different wire distances, i.e., $d_1 = 5$ mm, $d_2 = 20$ mm, are considered for simulation, in order to carry out the comparison for values of k satisfying (i.e., $k_2 = 0.3$) and not-satisfying (i.e., $k_1 = 0.56$) the weak-coupling condition $k^2 \ll 1$, [10], [11]. The obtained self, $y_{11} = y_{22}$, and mutual, $y_{12} = y_{21}$, admittances are shown on the left and right columns of Fig. 3. The plots on the first row were obtained assuming terminations of the generator circuit equal to the characteristic impedance Z_G, that is $\alpha = 1$. Conversely, those on the second and third rows were obtained for degrees of mismatching equal to $\alpha = 10$ and $\alpha = 0.1$, respectively. In each plot, black-dashed curves represent the entries of matrix $\boldsymbol{Y}_R$ in (15). Solid and dotted curves are used for the entries of matrices $\boldsymbol{Y}$ in (14) and $\boldsymbol{Y}_{XT}$ in (21)–(22). Among these, red and blue curves were obtained for coupling coefficient satisfying (k_2) and not satisfying (k_1) the weak-coupling condition, respectively. The proposed comparison shows that in the absence of weak coupling (see blue curves), the entries of $\boldsymbol{Y}_{XT}$ in (21)–(22) are strictly negligible only for $\alpha = 10$, i.e., for very large impedances at terminations of the generator circuit. Conversely, discrepancies of some decibels are observed between the entries of matrix $\boldsymbol{Y}$ and $\boldsymbol{Y}_R$ for $\alpha = 1$ (mainly in y_{11}) and for $\alpha = 0.1$ (mainly in y_{12}). However, if the assumption of weak coupling is satisfied, these discrepancies become negligible (since the entries of matrix $\boldsymbol{Y}_{XT}$ result to be much smaller than the corresponding entries of $\boldsymbol{Y}_R$, with the exception of narrow frequency intervals around the minima), and crosstalk voltage and currents at the terminations of the receptor can be approximately predicted by neglecting matrix $\boldsymbol{Y}_{XT}$ in (14), without restrictive assumptions on the loads at the terminations of the victim circuit.

3. Conditions of Equivalence with FC

3.1 Enforcing Equivalence of the Active Part

As long as perturbation of the passive part is negligible,

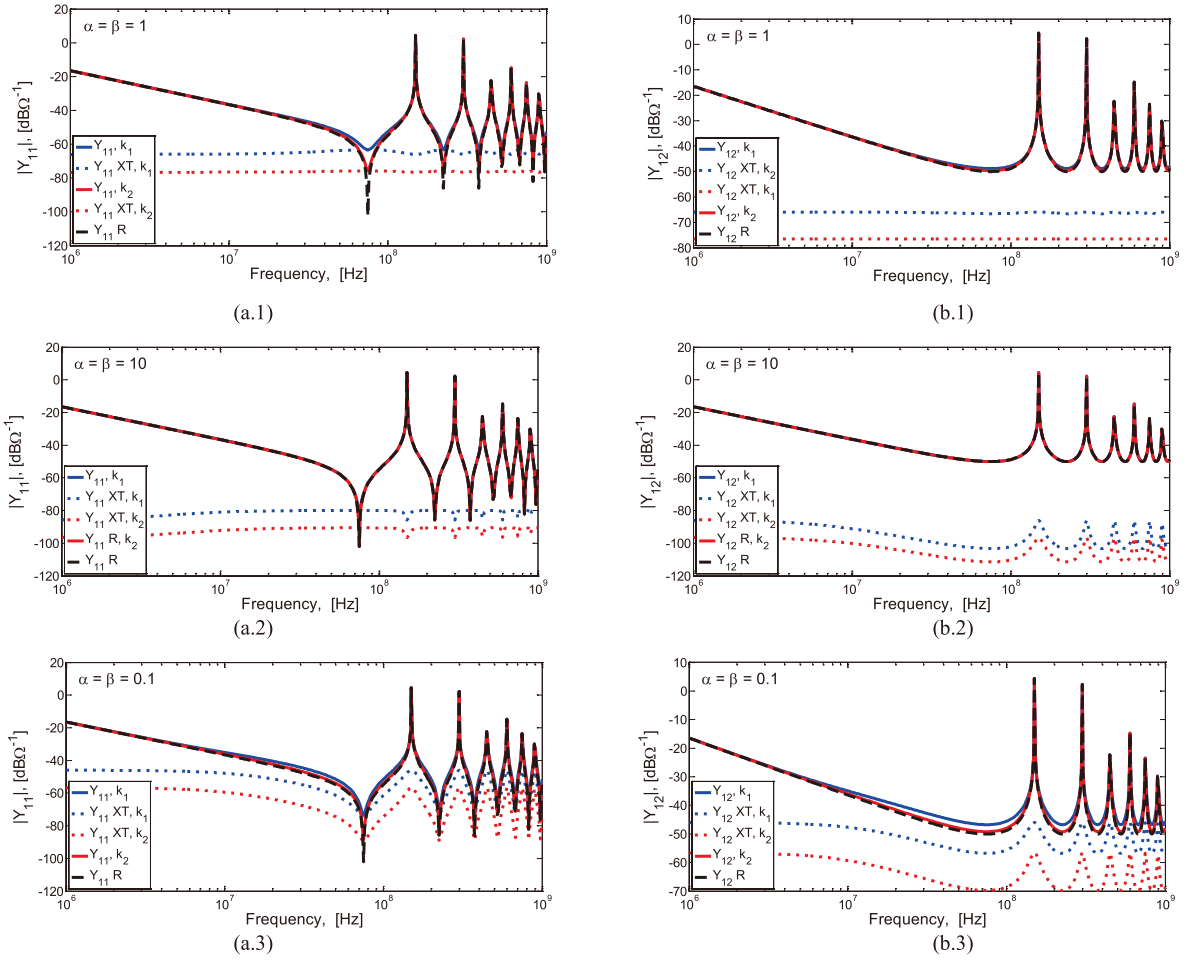

Fig. 3 Comparison of the entries of matrices $\boldsymbol{Y}$, $\boldsymbol{Y}_R$, $\boldsymbol{Y}_{XT}$ for different degrees of mismatching of the generator circuit.

equivalence with FC can be achieved by enforcing equivalence of the active part of the two models. To this end, the voltage sources in (12)–(13) are preliminary simplified by the assumption $\beta = \alpha$, and subsequently compared to the voltage sources V_{FC0} and V_{FCL} induced by FC (see Appendix). Apart for specific incidence conditions [5], the use of two RF sources feeding the generator circuit from both terminations (as shown in Fig. 4) is in general required, [4]. Namely, in the presence of this new generator circuit ($\alpha = \beta$), XT-induced sources V_{XT0}, V_{XTL} take the analytical expressions:

$$\tilde{V}_{XT0} = \frac{Z_m}{Z_G} \frac{[\alpha \cosh(\gamma_0 \ell) + \sinh(\gamma_0 \ell)]V_{S1} + \alpha V_{S2}}{2\alpha \cosh(\gamma_0 \ell) + (1+\alpha^2)\sinh(\gamma_0 \ell)}, \quad (23)$$

$$\tilde{V}_{XTL} = \frac{Z_m}{Z_G} \frac{\alpha V_{S1} + [\alpha \cosh(\gamma_0 \ell) + \sinh(\gamma_0 \ell)]V_{S2}}{2\alpha \cosh(\gamma_0 \ell) + (1+\alpha^2)\sinh(\gamma_0 \ell)}, \quad (24)$$

and can be made equivalent to those induced by FC for whatever combination of wave angles. This leads to the following analytical expressions for the voltage sources V_{S1} and V_{S2} in Fig. 4:

$$V_{S1} = \frac{Z_G}{Z_m} \frac{[\alpha \cosh(\gamma_0 \ell) + \sinh(\gamma_0 \ell)]V_{FC0} - \alpha V_{FCL}}{\sinh(\gamma_0 \ell)}, \quad (25)$$

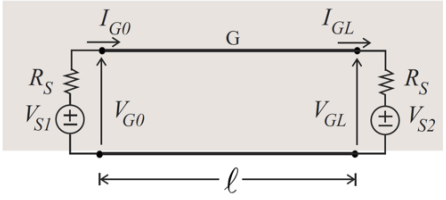

Fig. 4 Principle drawing of the generator circuit exploited to assure equivalence with FC.

$$V_{S2} = \frac{Z_G}{Z_m} \frac{[\alpha \cosh(\gamma_0 \ell) + \sinh(\gamma_0 \ell)]V_{FCL} - \alpha V_{FC0}}{\sinh(\gamma_0 \ell)}. \quad (26)$$

It's worth noting that validity of previous expressions is not limited to values of k assuring weak coupling, since the only assumption exploited for the derivation of (25)–(26) from (12)–(13) was $\alpha = \beta$.

3.2 Practical Implementation

Without lack of generality, validity of the proposed equivalence scheme will be proven with reference to typical test

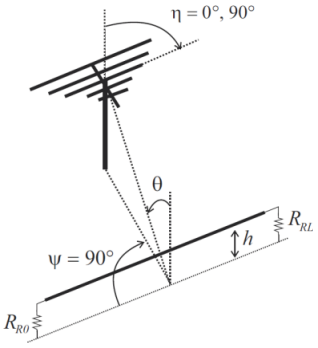

Fig. 5 RS test setup foreseen by aerospace EMC Standards, [7], [8].

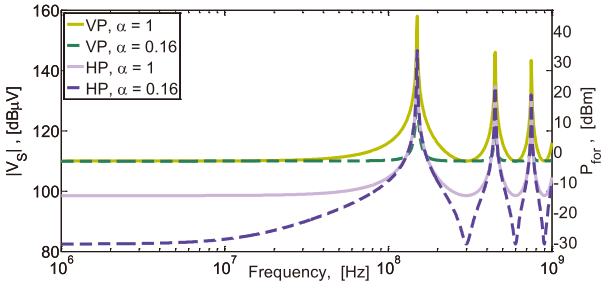

Fig. 6 Matched ($\alpha = 1$) vs unmatched ($\alpha = 0.16$) generator circuit: Feeding profiles, $|V_S| = |V_{S1}| = |V_{S2}|$, required for VP and HP of the antenna.

setups and incidence conditions foreseen by aerospace EMC Standards [7], [8]. According to these requirements, the sub-system under test (typically two units interconnected by a cable bundle) shall be placed at a constant height h above ground and illuminated by an antenna pointed towards the middle of the cable harness. A principle drawing of the test setup is shown in Fig. 5. In this configuration, the field generated by the antenna can be approximated as a plane-wave field characterized by (see Fig. 5) azimuth angle $\psi = 90°$, and polarization angle η equal to 0° or 90° depending on antenna polarization, that is: $\eta = 0°$ for vertical polarization (VP), and $\eta = 90°$ for horizontal polarization (HP). Concerning the elevation angle θ, it depends on the reciprocal distance between the wiring harness and the antenna tip. Hence, it will be treated as a variable parameter.

3.2.1 Vertical Polarization

For VP, the sources induced by FC, i.e., V_{FC0} and V_{FCL} in Fig. A· 1, are equal each other and take the simplified expression: $V_{FC0} = V_{FCL} = -2E_0 h \sin(\theta)$. Therefore, also the two RF sources feeding the generator circuit are equal in magnitude and phase, and can be expressed as:

$$V_{S1} = V_{S2} = -\frac{2E_0 h \sin(\theta) Z_G}{Z_m}\left[1 + \alpha \frac{\cosh(\gamma_0 \ell) - 1}{\sinh(\gamma_0 \ell)}\right], \tag{27}$$

where E_0 denotes the strength of the electric-field vector.

3.2.2 Horizontal Polarization

For HP, the sources induced by FC at the terminations of the receptor circuit take the analytical expressions:

$$V_{FC0} = 2E_0 h \cos(\theta) \frac{1 - \cosh(\gamma_0 \ell)}{\sinh(\gamma_0 \ell)}, \quad V_{FCL} = V^*_{FC0}, \tag{28}$$

where V^*_{FC0} denotes the complex conjugate of V_{FC0}. Hence, under the simplifying assumption of negligible losses, the two sources induced by FC are pure imaginary numbers equal in magnitude but opposite in phase, i.e., $V_{FCL} = -V_{FC0}$. It follows that also the two RF generators feeding the generator circuit should be equal in magnitude but opposite in phase, and can be expressed as function of V_{FC0} in (28) as:

$$V_{S1} = -V_{S2} = \frac{Z_G}{Z_m}\left[1 + \alpha \frac{\cosh(\gamma_0 \ell) + 1}{\sinh(\gamma_0 \ell)}\right] V_{FC0}. \tag{29}$$

3.2.3 Matched vs Unmatched Generator Circuit

For the geometrical dimensions considered in Sect. 2.2 (here the line-to-line distance $d_2 = 20\,\text{mm}$ was chosen to satisfy the weak coupling assumption), the magnitude of the feeding profiles in (27), (29) is shown in Fig. 6 (here, the elevation angle θ was set to the value: $\theta = 73°$). Two different test cases are considered. In the first test case, the terminations of the generator circuit are matched (i.e., $\alpha = \beta = 1$). In the second test case, the practically-relevant case of RF generators with internal resistance $50\,\Omega$ (i.e., $R_S = R_L = 50\,\Omega$), leading to values of $\alpha = \beta \approx 0.16$, is considered.

At low frequency, the magnitude of the two RF generators, i.e., $|V_S|$, exhibits a flat frequency behavior for both polarizations, which can be approximated as:

$$|V_S|^{VP} = 2Z_G Z_m^{-1} h E_0 \sin(\theta), \tag{30}$$

$$|V_S|^{HP} = 2Z_G Z_m^{-1} h E_0 \alpha \cos(\theta). \tag{31}$$

The comparison between VP and HP in (30) and (31), respectively, puts in evidence (a) the complementary dependence on the elevation angle θ, and (b) the different dependence on the degree of mismatching ($\alpha = \beta$) of the generator circuit. Concerning the first aspect, the comparison of the solid curves in Fig. 6 shows that the feeding profiles required for the two polarizations are just shifted the one with respect to the other by a factor which depends on the elevation angle θ. Concerning dependence on the degree of mismatching of the generator circuit, the observed independence of VP and proportionality of HP to α play a role on the overall level of forward power required for practical implementation of the test. As a matter of fact, comparison of the plots in Fig. 6 shows that the forward power (see y-scale on the right) required for the test, i.e., $P_{for} = |V_S|^2/(4R_{in})$ with $R_{in} = 50\,\Omega$, is expected to be generally lower when the impedances at the terminations of the generator circuit take the practical relevant value $R_S = 50\,\Omega$ (i.e., standard internal impedance of RF generators, leading to $\alpha = \beta \approx 0.16$), rather than in

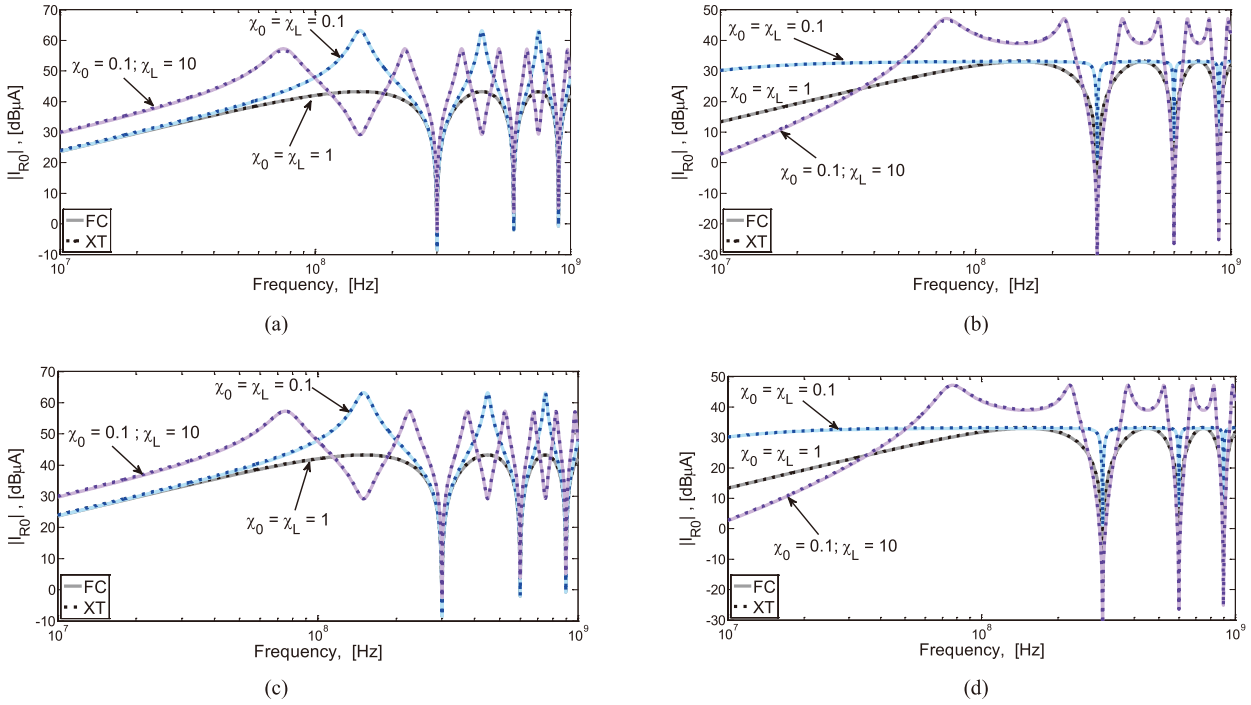

Fig. 7 TL-based prediction of the current induced at the receptor left end by FC (solid) and XT (dotted) for VP [plots (a), (c)] and HP [plots (b), (d)] and for different degrees of mismatching (χ_0, χ_L) of the receptor: Matched [plots (a), (b)] vs unmatched [plots (c), (d)] generator circuit.

the case of matching.

4. Validation of the Proposed Scheme of Equivalence

4.1 Preliminary Validation Based on TL Theory

The proposed scheme of equivalence was preliminary validated by comparing the current induced at the terminations of the victim circuit by FC and XT as predicted by TL-based modeling of the two test setups. For XT simulation, two bare wires [with $r_w = 0.5\,\text{mm}$, $\ell = 1\,\text{m}$, $h = 20\,\text{mm}$] separated by a distance $d_2 = 20\,\text{mm}$ (weak-coupling) are considered. For FC simulation, the victim circuit [i.e., a bare wire with $r_w = 0.5\,\text{mm}$, $\ell = 1\,\text{m}$, $h = 20\,\text{mm}$] is assumed to be illuminated by a uniform plane wave characterized by: $E_0 = 1\,\text{V/m}$, $\psi = 90°$, $\theta = 73°$, and polarization angle $\eta = 0°$ (VP), $\eta = 90°$ (HP). Simulation results (i.e., currents induced at the left termination of the receptor) are plotted in Fig. 7 for different degrees of mismatching at the terminations of the victim circuit (i.e., for different values of coefficients $\chi_0 = R_{R0}/Z_R$, $\chi_L = R_{RL}/Z_R$, where R_{R0} and R_{RL} denote the impedances at the left and right ends, respectively). The remarkable agreement between solid (FC) and dotted (XT) curves confirms the validity of the proposed scheme of equivalence both in the case of matched (i.e., $R_S = Z_G$, first row) and unmatched (i.e, $R_S = 50\,\Omega$, second row) terminations of the generator circuit.

4.2 Virtual Experiments

For virtual experiments, full-wave simulations of the FC and XT test setups described in the previous paragraph were carried out by the MoM-based software Feko, [9]. To this end, the horizontal wires were subdivided into 100 segments of length 1 cm, whereas five segments of length 4 mm each were used to realize the vertical risers. Sources and loads (lumped elements) were located at the bottom of the vertical risers. To ease simulation of the XT setup, system linearity was exploited. Namely, two frequency-independent sources with unitary amplitude and phase shift equal to 0° (VP) and 180° (HP) were exploited, and the obtained currents afterwards multiplied by the required feeding profiles. The obtained results (currents induced at the left termination of the receptor circuit) are plotted in Fig. 8, and exhibit an appreciable agreement both in the case of matched (i.e., $R_S = Z_G$) and unmatched (i.e., $R_S = 50\,\Omega$) generator circuit. Few discrepancies are observed only in narrow intervals around the frequencies in which the feeding profiles in Fig. 6 exhibit peaks of theoretically-infinite value (for practical implementation of the test, the amplitude of these peaks shall be reduced on the basis of the allowable range of variation of the output of the involved RF generators and amplifiers). At these frequencies, XT-induced currents exhibit spurious peaks that are to be ascribed to the effect of the vertical risers, whose contribution (which anyway depends on the specific realization of the riser) was neglected in the derivation of the

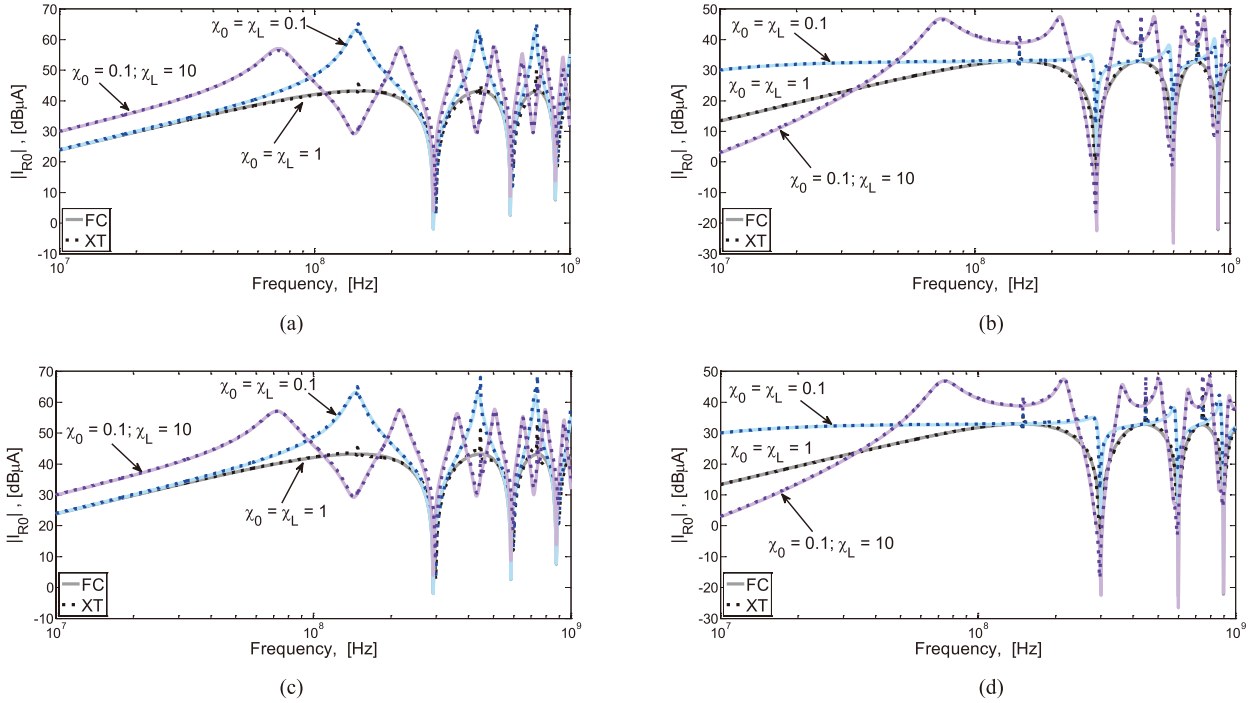

Fig. 8 Feko simulation of the current induced at the receptor left end by FC (solid) and XT (dotted) for VP [plots (a), (c)] and HP [plots (b), (d)] and for different degrees of mismatching (χ_0, χ_L) of the receptor: Matched [plots (a), (b)] vs. unmatched [plots (c), (d)] generator circuit.

proposed equivalence scheme.

5. Conclusion

In this work, a novel formulation of crosstalk was proposed, which allowed verification of the idea that, as long as the weak-coupling assumption is satisfied, the previously identified [4] condition of matching of the generator circuit is not strictly necessary to assure negligibility of the perturbation this circuit exerts on the passive part of the receptor. On the basis of the obtained results, an equivalence scheme assuring equivalence between XT and FC in terms of voltages/currents induced at the receptor ends was formulated and validated by virtual experiments with reference to the RS test setup foreseen by aerospace Standards, [7], [8]. With respect to the matched case [4], it was proven that the practically-relevant case of terminations of the generator circuit equal to 50 Ω (standard input impedance of RF generators) (a) provides comparable accuracy in the reconstruction of FC voltages/currents at the receptor-ends; and (b) offers advantages in terms of reduction of the forward power required for the test.

Without the pretension to avoid RS verification in field chambers (also because the proposed XT-based test can only reproduce the effects of FC with external harnesses), the analysis here presented validates the idea to exploit XT to develop a test-bench procedure assuring high correlation with FC and not requiring exact knowledge on the terminal units, as in [2], [3]. Undoubtedly, several aspects have still to be investigated in view of practical implementation. First, proper design of the generator circuit, possibly exploiting power amplifiers to reproduce the required field strengths (e.g., from 1 to 10 V/m in [8]), and a well-controlled test setup as, for instance, the parallel-wire fixture foreseen in [13]. Second, extension of the analysis to victim circuits comprising complex wiring harnesses, with the more practical objective to derive approximate feeding conditions for the involved RF sources, assuring high correlation, rather than exact reproduction (as it was done here), with FC effects.

References

[1] C.R. Paul, "The concept of dominant effect in EMC," IEEE Trans. Electromagn. Compat., vol.34, no.3, pp.363–367, Aug. 1992.
[2] D.A. Hill, "Currents induced on multiconductor transmission lines by radiation and injection," IEEE Trans. Electromagn. Compat., vol.34, no.4, pp.445–450, Nov. 1992.
[3] J.W. Adams, J. Cruz, and D. Melquist, "Comparison measurements of currents induced by radiation and injection," IEEE Trans. Electromagn. Compat., vol.34, no.3, pp.360–362, Aug. 1992.
[4] F. Grassi, H. Abdollahi, G. Spadacini, S.A. Pignari, and P. Pelissou, "Radiated immunity test involving crosstalk and enforcing equivalence with field-to-wire coupling," IEEE Trans. Electromagn. Compat., vol.58, no.1, pp.66–74, Feb. 2016.
[5] S.A. Pignari and F. Grassi, "Crosstalk-based radiated susceptibility test," Electron. Lett., vol.40, no.22, pp.1398–1399, Oct. 2004.
[6] S.A. Pignari and F. Grassi, "An alternative approach to radiated susceptibility testing of airborne equipment," Proc. 2010 Asia-Pacific International Symposium on Electromagnetic Compatibility, pp.548–551, 2010.
[7] RTCA-EUROCAE, Environmental Conditions and Test Procedures for Airborne Equipment, Section 20: Radio Frequency Susceptibility

(Radiated and Conducted), RTCA DO-160F, Dec. 2007.
[8] European Cooperation for Space Standardization, Space Engineering Electromagnetic Compatibility, ECSS-E-20-07A, Feb. 2008.
[9] FEKO Suite 6.3 User's Manual (Oct. 2013), © EM Software and Systems, Stellenbosch, South Africa, www.feko.info
[10] C.R. Paul, Introduction to Electromagnetic Compatibility, Wiley, NewYork, 1992.
[11] C.R. Paul, "Solution of the transmission-line equations under the weak-coupling assumption," IEEE Trans. Electromagn. Compat., vol.44, no.3, pp.413–423, Aug. 2002.
[12] A.K. Agrawal, H.J. Price, and S.H. Gurbaxani, "Transient response of multiconductor transmission lines excited by a nonuniform electromagnetic field," IEEE Trans. Electromagn. Compat., vol.EMC-22, no.2, pp.119–129, May 1980.
[13] Ford Motor Company, EMC Specification for Electrical/Electronic Components and Subsystems, EMC-CS-2009.1, Sections 13, 14: Coupled Immunity: RI 130, RI 150, Feb. 2010.

Appendix:

As far as prediction of currents and voltages induced by a uniform plane wave at the terminations of a two-conductor TL above ground is the target, effects due to the interfering field can be represented by lumped voltage sources connected to the terminations of the victim TL [here represented by the admittance matrix $\boldsymbol{Y}_R$ in (14)] as shown in Fig. A· 1, [12]. Analytical expressions for these sources as function of the wave angles defined in Fig. 5 can be found in [4], and are not repeated here for the sake of brevity. For the specific incidence conditions of interest for this work (so-called *broadside incidence*, [10]), simplified expressions are reported in Sect. 3.2.1 (VP) and Sect. 3.2.2 (HP).

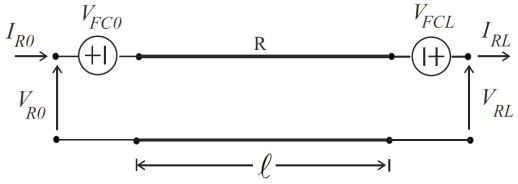

Fig. A· 1 Open-ended representation of the victim/receptor circuit with FC effects included by means of two induced voltage sources.

Flavia Grassi received the Laurea and Ph.D. degrees in electrical engineering from the Politecnico di Milano, Italy, in 2002 and 2006, respectively, where she is currently an Assistant Professor with the Department of Electronics, Information and Bioengineering. From 2008 to 2009, she was with the European Space Agency (ESA), The Netherlands. Her research interests are focused on the characterization of measurement setups for electromagnetic compatibility testing (aerospace and automotive sectors), and applications of the powerline communications (PLC) technology on ac and dc lines. Dr. Grassi was awarded the IEEE Young Scientist Award at the 2016 Asia-Pacific Int. Symp. on Electromagnetic Compatibility (EMC). She was a recipient of the 2016 IEEE EMC Transactions Prize Paper Award.

Giordano Spadacini received the Laurea (M.S.) and Ph.D. degrees in electrical engineering from the Politecnico di Milano, Milan, Italy, in 2001 and 2005, respectively. Since 2007 he has been an Assistant Professor at the Politecnico di Milano, Department of Electronics, Information and Bioengineering. His research interests include distributed-parameter circuit modeling, statistical models for the characterization of interference effects, and EMC in railway and aerospace systems. Dr. Spadacini received two Best EMC-Transactions Paper Awards for articles published in 2004 and 2015.

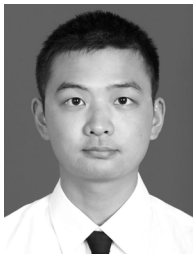

Keliang Yuan received the B.S. degree in engineering physics from Tsinghua University, Beijing, China, in 2012, where he is currently working toward the Ph.D. degree in engineering physics. His current research interests include electromagnetic compatibility and transmission-line analysis. From Sept. 2015, he started his exchange mobility in the EMC research group in the Department of Electronics, Information and Bioengineering, Politecnico di Milano.

Sergio A. Pignari received the Laurea and Ph.D. degrees in electronic engineering from the Politecnico di Torino, Turin, Italy, in 1988 and 1993, respectively. From 1991 to 1998, he was an Assistant Professor with the Department of Electronics, Politecnico di Torino, Turin, Italy. In 1998, he joined Politecnico di Milano, Milan, Italy, where he is currently a Full Professor of Circuit Theory and Electromagnetic Compatibility (EMC) with the EMC Group, at the Department of Electronics, Information, and Bioengineering. His current research interests include characterization of interference effects, distributed parameter circuit modeling, statistical techniques for EMC, and experimental procedures and setups for EMC testing. Dr. Pignari is a recipient of the 2005 and 2016 IEEE EMC Society Transactions Prize Paper Award. He is an IEEE Fellow and an Associate Editor of the IEEE Transactions on Electromagnetic Compatibility.